Talanta 114 (2013) 43–48

Contents lists available at ScienceDirect

Talanta

journal homepage: www.elsevier.com/locate/talanta

Electrochemical biosensor based on silver nanoparticles–polydopamine–graphene nanocomposite for sensitive determination of adenine and guanine

Ke-Jing Huang *, Lan Wang, Hai-Bo Wang, Tian Gan, Ying-Ying Wu, Jing Li, Yan-Ming Liu *

College of Chemistry and Chemical Engineering, Xinyang Normal University, Xinyang 464000, China

ARTICLE INFO

Article history:
Received 17 January 2013
Received in revised form
29 March 2013
Accepted 6 April 2013
Available online 12 April 2013

Keywords:
Ag nanoparticles–polydopamine@graphene nanocomposite
Adenine
Guanine
Electrochemical sensor
Voltammetry
Biosensing

ABSTRACT

A multifunctional Ag nanoparticles (AgNPs)–polydopamine (Pdop)@graphene (Gr) composite was prepared by a simple and mild procedure. Gr was easily coated with Pdop at room temperature and then AgNPs was deposited by mildly stirring. The nanocomposite was characterized by scanning electron microscope (SEM) and transmission electron microscope (TEM). Guanine and adenine as model moleculars were employed to study their electrochemical responses at the Ag–Pdop@Gr composite modified electrode, which showed more favorable electron transfer kinetics than Gr modified glassy carbon and AgNPs modified glassy carbon electrodes. The Ag–Pdop@Gr modified electrode exhibited linear ranges of 0.04–50 μM and 0.02–40 μM with detection limits of 4.0 nM and 2.0 nM for guanine and adenine, respectively. The developed method was applied for simultaneous determination of trace-level adenine and guanine in fish sperm. The results demonstrated that the AgNPs–Pdop@Gr nanocomposite was a promising substrate for the development of high-performance electrocatalysts for biosensing.

1. Introduction

Guanine and adenine are important components found in deoxyribonucleic acid and play fundamental roles in life process. They have widespread effects on coronary and cerebral circulation, prevention of cardiac arrhythmias and inhibition of neurotransmitter release [1]. Therefore, the determination of guanine and adenine has great significance to the bioscience and clinical diagnosis.

Electrochemical method has been widely used in the determination of guanine and adenine [2]. However, the low concentrations in biosamples and the complexity of their matrices make determination of guanine and adenine challenging tasks. It is very important to explore new method for signal amplification in order to increase the sensitivity of the detection. Several methods for signal enhancement have been investigated, such as enzyme labeling [3], rolling circle amplification [4] and nanomaterial introduction [5,6]. Among these methods, application of nanomaterial has gained growing interest due to the intrinsic advantages of nanomaterials, such as low cost, good thermal stability and large surface area.

Graphene (Gr) has stimulated intense research interest because of its unique physical and chemical properties, such as high surface area, high electrical conductivity, good chemical stability, and strong mechanical strength [7]. These properties make it an attractive candidate for fabricating various functional devices, such as electrodes, sensors, photovoltaics and photodetectors [8,9]. Silver nanoparticles (AgNPs) have good conductivity and high electrochemical catalytic activity. The availability of AgNPs will expand the possibilities for the preparation of Ag-doped nanomaterials and extend its application in biosensor [10]. It has been reported that the integration of carbon-based materials and metal nanoparticles usually shows synergistic effects in electrocatalytic applications [11], so there is a reason to expect the integration of Gr and AgNPs will obtain the similar effect on the electrooxidation of guanine and adenine.

Recently, a thin, surface adherent and multifunctional biopolymer–polydopamine (Pdop) layer was prepared on a wide range of inorganic and organic materials by self-polymerization of dopamine in an aqueous solution [12]. A variety of ad-layers, including self-assembled monolayer through deposition of long-chain molecular building blocks, metal films by electroless metallization and bioactive surfaces via grafting of macromolecules have been prepared by Pdop coating [13]. The polymerization of dopamine offers the advantage of a one-step surface functionalization and allows the introduction of a new paradigm in the field of surface

* Corresponding authors. Tel.: +86 376 6390611.
E-mail addresses: kejinghuang@163.com (K.-J. Huang), liuym9518@sina.com (Y.-M. Liu).

0039-9140/$ - see front matter © 2013 Elsevier B.V. All rights reserved.
http://dx.doi.org/10.1016/j.talanta.2013.04.017

modification. In this work, a new multifunctional Ag nanoparticles (AgNPs)–polydopamine (Pdop)@graphene (Gr) composite was firstly prepared through the oxidation of dopamine on Gr at room temperature and subsequent electroless silver deposition by mildly stirring. The AgNPs–Pdop@Gr modified glassy carbon electrodes (GCE) showed enhanced catalytic efficiencies towards guanine and adenine oxidation in acetate buffer solution.

2. Experimental

2.1. Chemicals and materials

Graphite powder, hydrazine solution (50 wt%) and ammonia solution (28 wt%) were purchased from Shanghai Chemical Reagent Corporation (Shanghai, China). Guanine, adenine, $AgNO_3$, dopamine hydrochloride (DA) and 2-amino-2-hydroxymethylpropane-1,3-diol (Tris) were obtained from Sigma (Saint Louis, MO, USA). Acetate buffer solutions (ABS) were prepared by mixing of 0.1 M CH_3COOH and CH_3COONa and adjusting the pH with NaOH. All chemicals were of analytical grade and doubly distilled water was used throughout.

2.2. Apparatus

Electrochemical measurements were performed on a CHI 660D Electrochemical Workstation (Shanghai CH Instruments, China). A conventional three-electrode system was used throughout the experiments. The working electrode was a bare, a pretreated or AgNPs–Pdop–Gr composite modified GCE (3.0 mm in diameter); the auxiliary electrode was a platinum wire and a saturated calomel electrode (SCE) was used as the reference. Electrochemical impedance spectroscopy (EIS) was performed in 5.0 mM $K_3Fe(CN)_6/K_4Fe(CN)_6$ (1/1) mixture with 0.1 M KCl as supporting electrolyte, using an alternating current voltage of 5 mV, within the frequency range of 0.1–10^5 Hz by Autolab Electrochemistry Instruments (Autolab, Eco Chemie, The Netherlands). The morphologies of the nanocomposite were recorded on a JEM 2100 transmission electron microscope (TEM) and a Hitachi S-4800 scanning electron microscope (SEM).

2.3. Preparation of graphene and its functionalized products

Graphene oxide (GO) was prepared from graphite powder by the modified Hummers method [14]. In a typical process, 5 g graphite was slowly added into a mixture of concentrated H_2SO_4 (87.5 mL) and fuming HNO_3 (45 mL) (warning: concentrated H_2SO_4 and fuming HNO_3 are strongly oxidizing and should be handled with care!). $KClO_3$ (55 g) was then added in above mixture, and was kept stirring for 96 h. Then the slurry was poured into water and filtered to obtain graphite oxide. After dried at 80 °C, graphite oxide (0.5 g) was exfoliated in 500 mL water with ultrasonic treatment to form a colloidal graphene oxide suspension (1 mg mL^{-1}). To get Gr, chemical reduction of the suspension of GO was carried out with hydrazine monohydrate for 24 h at 80 °C. The final product was isolated by filtration, and rinsed thoroughly with pure water and ethanol. Then the product was dried in vacuum and Gr was obtained.

AgNPs–Pdop–Gr nanocomposite was prepared as following: 100 mg Gr was dispersed in 100 mL water by sonication, then 200 mg DA and 120 mg Tris were added into above mixture and dispersed by 1 min sonication in ice water bath. The mixture was magnetically stirred at room temperature for 20 h. The product were filtered, washed and then dried in vacuum overnight at 60 °C to obtain Pdop@Gr. To mildly deposit AgNPs onto the surface of Pdop@Gr, 25.0 mL $AgNO_3$ aqueous solution (1.0 mM) was added in 25.0 mg Pdop@Gr. The mixture was mildly stirred for 2 h at room temperature, and then the product was filtered, washed and dried in vacuum overnight at 60 °C to obtain AgNPs–Pdop@Gr nanocomposite.

2.4. Preparation of Ag–Pdop@gr modified GCE

For electrode preparation, 1 mg AgNPs–Pdop@Gr was dispersed in 10 mL DMF using an ultrasonic bath to give a black suspension. The GCE (3 mm in diameter) was polished carefully with 0.3 and 0.05 μm alumina slurry, and sonicated in water and ethanol, respectively. Then, 8 μL of the suspension was placed on the GCE surface by micropipette and left to dry at room temperature (30 min) to obtain AgNPs–Pdop@Gr/GCE. The Gr/GCE without AgNPs and AgNPs/GCE without Gr were also prepared according to the similar procedure, using a suspension of Gr and AgNPs in DMF. Before voltammetric measurements, the modified electrode was cycled five times between 0.5 and 1.4 V (scan rate 100 mV s^{-1}) in a 0.1 M ABS of pH 4.0. The renewal of the electrode surface was easily accomplished by soaking the modified electrode in ABS and cycling the potential as mentioned above.

2.5. Preparation of DNA samples

Thermally denatured dsDNA was prepared according to the previous report [15]. In short, 3 mg of the fish sperm DNA was digested using 1 mL of 1 M HCl in a sealed 10 mL glass tube. After heating in boiling waterbath (100 °C) for 80 min, 1 mL of 1 M NaOH was added. After cooling to room temperature, the solution was diluted to 10.0 mL using 0.1 M PBS (pH 7).

3. Results and discussion

3.1. Characterization

The morphology of the AgNPs–Pdop@Gr nanocomposite was examined by SEM and TEM. Fig. S1a showed the SEM image of the obtained Gr sheets, illustrating the flake-like shapes of graphene. Fig. S1b showed the SEM image of AgNPs–Pdop@Gr nanocomposite. It was clear that AgNPs distributed well on Pdop@Gr sheets, evidencing the well-behaved assembly process. The Pdop acted as a glue reagent connecting the Gr with AgNPs. Such morphological characteristics might result in high loading of guanine and adenine and fast response to the substrate. Fig. S1c showed the typical TEM image of the Gr nanosheets. Fig. S1d showed TEM image of the obtained Pdop@Gr. The transparent Gr turns into blackish nanosheets, illustrating Pdop was successfully coated on Gr. The TEM image (Fig. S1e) showed the AgNPs were deposited on the Gr surface. However, the size of these nanoparticles was not the same, and the dispersion was heterogeneous. The reason might be attributed to the stirring inhomogeneity of graphene nanosheets since the formation of silver nanoparticles was based on Pdop@Gr nanosheets as substrates. In fact, this was just an advantage over the composite surface for increasing the immobilized amount of the target molecules. These AgNPs were firmly attached to Gr sheets, even after the ultrasonication used to disperse the AgNPs–Pdop@Gr composite for TEM characterization. EDX measurement was performed to validate the presence of AgNPs on graphene (Fig. S1f).

3.2. Electrochemical reactivity

The capability of electron transfer of different electrodes was investigated by AC impedance experiments and the results were shown in Fig. S2. The sequence of the values of charge-transfer resistance for different electrodes was bare GC electrode (a,

742.6 Ω) > AgNPs/GCE (b, 627.3 Ω) > Gr/GCE (c, 498.2 Ω) > AgNPs–Pdop@Gr/GCE (d, 245.6 Ω). This result demonstrated the AgNPs–Pdop@Gr/GCE had higher electrochemical activity than other electrodes.

The potential window of the electrodes may have a deep impact upon their analytical applications. In Fig. S3, the potential window for the AgNPs–Pdop@Gr/GCE (d) in 0.1 M pH 4.0 ABS was ~2.75 V, which was comparable to that for bare GCE (a) and Gr/GCE (c) and better than that for AgNPs/GCE (b).

Fig. S4 depicted the chronocoulometric curves at different electrodes for the reduction of 1 mM $K_3Fe(CN)_6$ with 2 M KCl. According to the following equation:

$$Q = (2nFAD_o^{1/2}\pi^{-1/2}C_o)t^{1/2} \quad (1)$$

where Q is the absolute value of the reduction charge, n is the number of electrons for the reaction, F is the Faraday constant, A is the apparent electrode area, D_o is the diffusion coefficient of the oxidized form, hexacyanoferrate(III), C_o is the bulk concentration of the oxidized form, and t is the time. From the slope of the Q–$t^{1/2}$ line, the sequence of the values of A for different electrodes was AgNPs–Pdop@Gr/GCE (d) > Gr/GCE (c) > AgNPs/GCE (b) > GCE (a). This meaned the largest value of A was obtained on the AgNPs–Pdop@Gr/GCE, which may have the best electrochemical reaction ability among them.

The electrochemical response of the different modified electrodes was studied in the presence of $Fe(CN)_6^{3-/4-}$ (Fig. S5). $Fe(CN)_6^{3-/4-}$ is close to an ideal quasi-reversible system on carbon electrodes. For AgNPs–Pdop@Gr/GCE, the peak current showed the highest, which indicated that this well-defined AgNPs–Pdop@Gr film possessed the requisite surface structure and electronic properties to support rapid electron transfer for this particular mechanistically complicated redox system.

3.3. Electrocatalytic oxidation of guanine and adenine

The electrochemical behavior of guanine at different electrodes was studied in Fig. 1. The DPV of 1 μM guanine at an AgNPs–Pdop@Gr/GCE in 0.1 M ABS (pH 4.0) was shown in curve d. For comparison, a corresponding DPV was initially performed at a bare GCE and the result was depicted in curve a, which showed a broad oxidation peak with a rather weak intensity arising from slow electron transfer kinetics of the guanine oxidation process. However, an increasing oxidation peak was observed at AgNPs/GCE (curve b). This current peak was 1.7 times higher than that obtained at the bare GCE, indicating that AgNPs can efficiently facilitate the electron transfer involved in the oxidation of guanine. Moreover, compared to bare GCE, Gr/GCE exhibited 3.8 times increased peak current response (curve c). In the case of AgNPs–Pdop@Gr/GCE, 5.6 times enhancement of the peak current was obtained (curve d), suggesting that the catalytic capability of AgNPs–Pdop@Gr/GCE was higher than Gr/GCE. Such a large increase in catalytic activity for the oxidation of guanine can be attributed to compact dispersion of AgNPs on the Pdop@Gr assembly, resulting in an extraordinarily high effective surface area and very high electron transfer rate. Similarly, as shown in Fig. 2 and Fig. 3, the AgNPs/GCE and Gr/GCE also displayed strong electrocatalytic properties towards the oxidation of A and the simultaneous oxidation of guanine and adenine, while the highest electrocatalytic activities occurred at the AgNPs–Pdop@Gr/GCE.

The effect of buffer pH on the electrooxidation of guanine and adenine was also investigated in the range of pH 4.0–9.0. As shown in Fig. 4, the oxidation peak potential of G shifted positively with the decrease of pH (from 9.0 to 4.0), indicating the electrochemical oxidation of guanine was associated with a proton-transfer process. Linear relationships of the peak potential of guanine as function of solution pH with slopes of 58.0 $mVpH^{-1}$ were obtained, which was close to the expected Nernstian theoretical value of 59.1 mV pH^{-1} at 25 °C, suggesting that the uptake of electrons was accompanied by an equal number of protons. It was reported that the electrochemical oxidation of guanine followed a two-step mechanism involving the total loss of $4e^-$, and the first $2e^-$ oxidation was rate-determining step [16]. The slope of 58.0 mV pH^{-1} showed that two protons took part in the rate-determining step. In addition, the oxidation peak current of guanine increased gradually with the decrease of pH. Since the pKa of guanine was 2.4, most guanine molecules were protonated in acidic solution. Protonation was proved to involve in the catalytic reaction process, which was favorable for the oxidation of guanine [17]. With the decrease in pH, the electrocatalytic oxidation of guanine became easier due to the increase in proton, thus the catalytic peak current increased with the decrease in solution pH. So pH 4.0 ABS was selected for the following study. Similar phenomena can also be observed for the investigation of adenine (Fig. 4), and a good linear relation between the E_{pa} of adenine and the solution pH was obtained with a slope of 55.0 mV pH^{-1}.

The effect of scan rate was also investigated. The results showed that oxidation peak currents of guanine and adenine

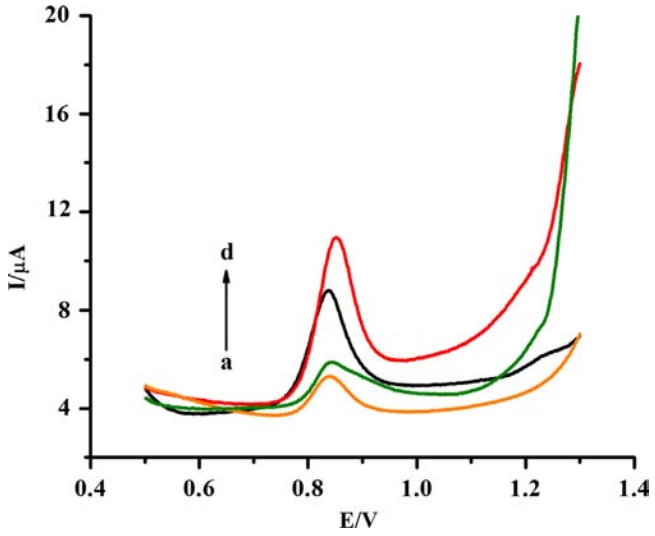

Fig. 1. DPVs of 1 μM guanine at bare GCE (a), AgNPs/GCE (b), Gr/GCE (c) and AgNPs–Pdop@Gr/GCE (d) in 0.1M pH 4.0 ABS.

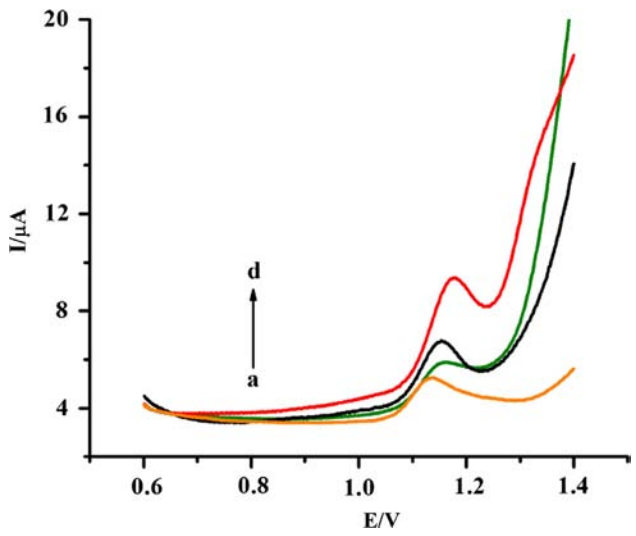

Fig. 2. DPVs of 0.1 μM adenine at bare GCE (a), AgNPs/GCE (b), Gr/GCE (c) and AgNPs–Pdop@Gr/GCE (d) in 0.1M pH 4.0 ABS.

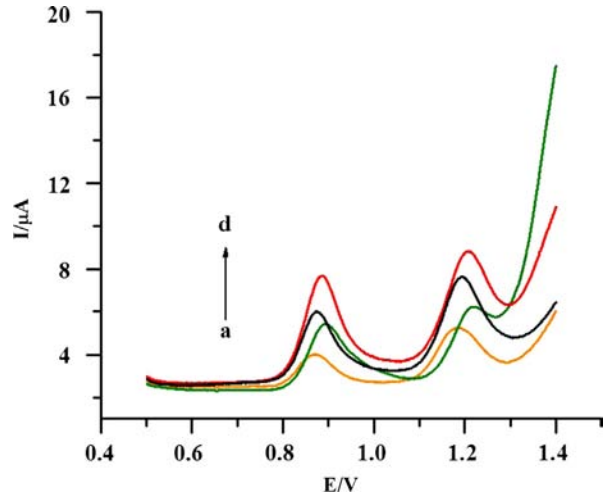

Fig. 3. DPVs of 1 μM guanine and 0.1 μM adenine at bare GCE (a), AgNPs/GCE (b), Gr/GCE (c) and AgNPs–Pdop@Gr/GCE (d) in 0.1M pH 4.0 ABS.

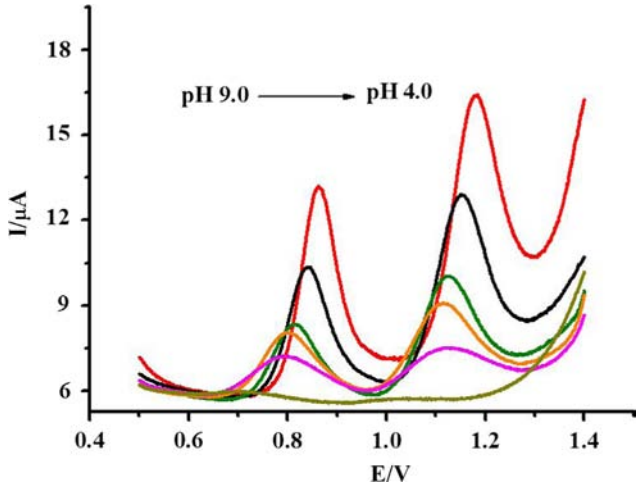

Fig. 4. DPVs of Ag–Pdop–GR/GCE in 0.1 M ABS containing 1.2 μM guanine and 0.2 μM adenine at different pH values (from bottom to top: pH 9.0, pH 8.0, pH 7.0, pH 6.0, pH 5.0, pH 4.0).

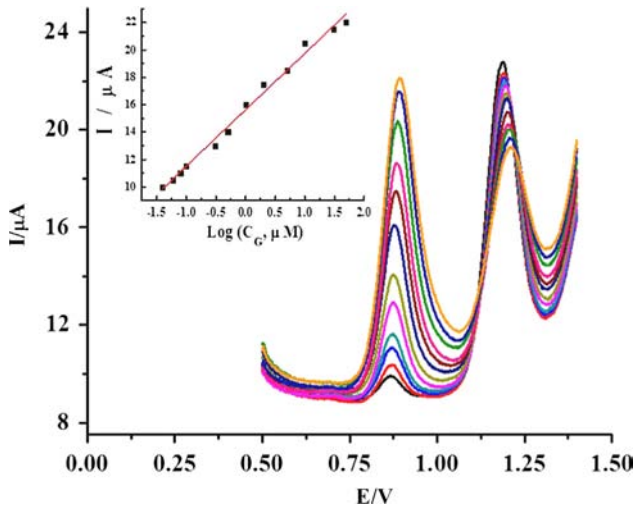

Fig. 5. DPVs of guanine at AgNPs–Pdop@Gr/GCE in the presence of 0.5 μM adenine in 0.1 M pH 4.0 ABS. Guanine concentrations (from bottom to top): 0.04, 0.06, 0.08, 0.1, 0.3, 0.5, 1, 2, 5, 10, 30, 50 μM. Insets are linear relationships between peak currents and concentrations.

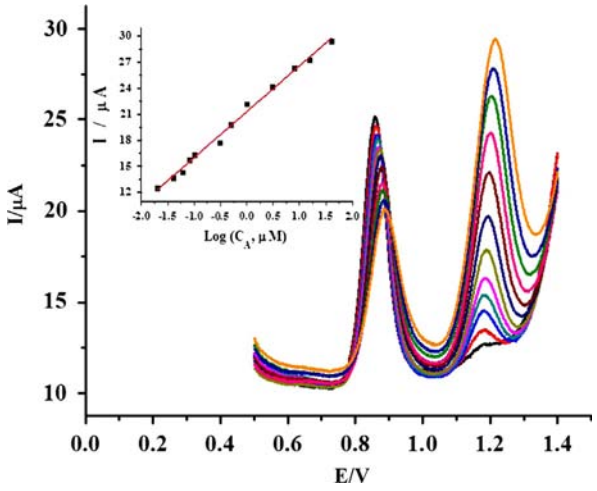

Fig. 6. DPVs of adenine at AgNPs–Pdop@Gr/GCE in the presence of 10 μM guanine, in 0.1 M pH 4.0 ABS. A concentrations (from bottom to top): 0.02, 0.04, 0.06, 0.08, 0.1, 0.3, 0.5, 1, 3, 8, 15, 40 μM. Insets are linear relationships between peak currents and concentrations.

increased linearly with the scan rate in the range of 20–300 mVs^{-1}, and the relationships between the oxidation peak currents and the scan rates were expressed as I_{pa} (μA)=0.18245 ν (mV s^{-1})+4.4621 (R=0.995) for adenine, I_{pa} (μA)=0.02587 ν (mV s^{-1})+1.5098 (R=0.992) for guanine. This indicates that the electro-oxidation reactions of guanine and adenine at the AgNPs–Pdop@Gr/GCE are surface-controlled process.

3.4. Determination of guanine and adenine

DPV was used for the determination of guanine and adenine at AgNPs–Pdop@Gr/GCE due to its high sensitivity. The individual determination of guanine or adenine in their mixtures was first investigated when the concentration of one species changed, whereas the other species remained constant. Fig. 5 showed the DPV curves of different concentration guanine in pH 4.0 ABS containing 0.5 μM adenine. As can be seen in the inset of Fig. 5, the I_{pa} was proportional to the logarithm of concentration of guanine in the range of 0.04–50 μM. The regression equation was I_{pa} (μA)=4.1149 log$C$+15.623 (R=0.9899), and the detection limit was 4.0 nM (S/N=3). Similarly, as shown in Fig. 6, keeping the concentration of guanine constant, the oxidation peak current increased linearly with increasing the logarithm of concentration of adenine in the range of 0.02–40 μM. A linear equation of I_{pa} (μA)=5.2929 log$C$+21.308 (R=0.9928) was obtained. The detection limit for adenine was 2 nM (S/N=3). Therefore, the proposed method can be used to simultaneously determine guanine and adenine.

In order to evaluate the feasibility of the AgNPs–Pdop@Gr/GCE for guanine and adenine determination, the fabricated electrode was applied to detect simultaneously guanine and adenine. As shown in Fig. 7, two well-defined oxidation peaks were observed at about 0.87 V and 1.19 V, corresponding to the oxidation of guanine and adenine, respectively. The oxidation peak currents of guanine and adenine increased linearly with the logarithm of their concentration in the range of 0.02–40 μM (I_{pa} (μA)=4.0461 log$C$+12.954, R=0.9921) for guanine and 0.02–40 μM (I_{pa} (μA)=4.5616 log$C$+14.498, R=0.9918) for adenine, respectively. The detection limits for guanine and adenine were 4.0 nM and 2 nM (S/N=3), respectively. Thus, the simultaneously sensitive determination of guanine and adenine was realized by using AgNPs–Pdop@Gr/GCE.

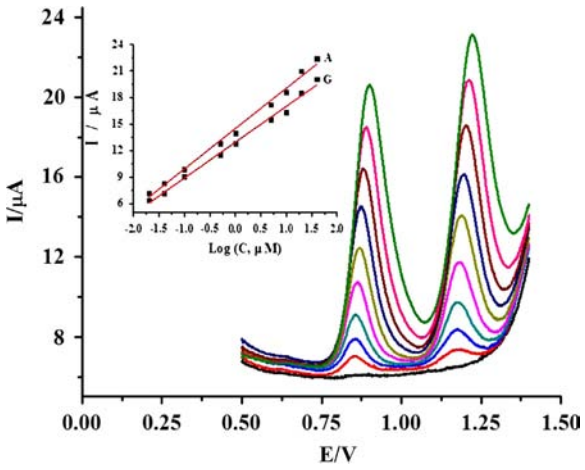

Fig. 7. DPVs of guanine and adenine at Ag–Pdop–GR/GCE in 0.1 M pH 4.0 ABS. Guanine and adenine concentrations (from bottom to top): 0.02, 0.04, 0.1, 0.5, 1, 5, 10, 20, 40 μM. Insets are linear relationships between peak currents and concentrations.

Table 1
Comparison of different electrochemical sensors for the determination of guanine and adenine.

Electrodes	Linear range (μM)		Detection limit (nM)		Reference
	Guanine	Adenine	Guanine	Adenine	
CILE[a]	0.3–50	1.5–70	78.7	250	[18]
PTH/NPAu/MWNTs[b]	0.05–5	0.05–5	10	8	[19]
MW-CNCE[c]	0.1–20	0.1–10	80	80	[20]
MWCNT/GCE[d]	0.05–10	0.05–10	20	80	[21]
TiO_2–Gr/GCE[e]	0.5–200	0.5–200	100	150	[2]
Fe_3O_4NPs/MWCNT/GCE[f]	0.01–10	0.05–6	1.0	5.0	[22]
AgNPs–Pdop@Gr/GCE	0.02–40	0.02–40	4.0	2.0	This work

[a] CILE: carbon ionic liquid on the carbon paste electrode.
[b] PTH/NPAu/MWNTs: poly thionine electrode deposited on GCE modified with gold nanoparticles/CNT.
[c] MW-CNCE: sol–gel-derived CNT ceramic electrode prepared by microwave irradiation.
[d] MWCNT/GCE: GCE modified with carboxylated MWCNTs.
[e] TiO_2–Gr/GCE:TiO_2 nanoparticles–graphene nanocomposite modified GCE.
[f] Fe_3O_4NPs/MWCNT/GCE: Fe_3O_4 nanoparticles–MWCNT modified GCE.

Table 1 compares the response characteristics of AgNPs–Pdop@Gr/GCE with other modified electrodes for the simultaneous determination of adenine and guanine [18–23]. The proposed method in this work had wide linear range and low detection limit. This further confirmed the synergetic effect of AgNPs and Gr.

3.5. Reproducibility, stability and interference

The reproducibility of the sensor was estimated by determining 1.0 μM guanine and 1.0 μM adenine with five modified electrodes which were made at the same electrode. Five measurements from the batch resulted in RSD of 4.1%. The experimental results showed good reproducibility of the fabrication protocol.

The stability of the developed sensor was evaluated by twenty successive scans in the mixture of 1.0 μM guanine and 1.0 μM adenine. The RSDs were found to be 2.4% and 2.5% for guanine and adenine, respectively, indicating excellent stability of the modified electrode. The longtime stability of the modified electrode was also studied on a 15-day period. The results showed that the analytical performance of the biosensor tested has no obvious decline (RSD≤5%).

The selectivity of the developed sensor for sensitive determination of guanine and adenine was analyzed and several compounds such as important biological substances and some metal ions were checked as potential interfering substances. The effects of these interferents were examined by carrying out the determination of 5 μM guanine and 3 μM adenine in 0.1 M ABS (pH 4.0) in the presence of different concentrations of the interferents. The tolerance limit was defined as the maximum concentration of the foreign substances that caused an approximately 5% relative error in the detection. The results suggested that 100-fold concentration of K^+, Na^+, Ca^{2+}, Mg^{2+}, Fe^{3+}, Al^{3+}, Zn^{2+}, Cl^-, NO_3^-, SO_4^{2-}, CO_3^{2-}, F^-, Br^-, glucose and cysteine had no interference for the determination of guanine and adenine. Ascorbic acid, uric acid and dopamine showed oxidation process in the selected potential range, but the oxidation potentials were lower than those of guanine and adenine. Furthermore, the peak current change of guanine and adenine was below 3%.

3.6. Analytical application

Because the bases are embedded in the interior of the double helix and therefore their detection is sterically hindered due to the crowded phosphate group on the exterior of the helix. The thermally denatured treatment results in an unwinding of duplex DNA and renders the guanine and adenine residues more accessible to the electrode surface owing to the increased flexibility in its structure. In this work, the applicability of the modified electrode in biological samples was assessed by measuring adenine and guanine in thermally denatured DNA. The thermally denatured DNA gave two well-defined oxidation peaks at the modified electrode, which was due to the oxidation of guanine and adenine residues, respectively. The standard addition methods were used to determine guanine and adenine. In short, 50 μL of thermally denatured DNA solution was added in a 10-mL buffer solution and the peak currents of the guanine and adenine were measured. Subsequently, 10 μM guanine and adenine were added in above mixture and the peak currents of the guanine and adenine were recorded again. From the differences between the peak currents of guanine and adenine, the concentration of guanine and adenine in DNA could be obtained by the calibration graph. The contents of guanine and adenine in thermally denatured DNA were calculated as 21.9% and 28.1% (in the molar ratio, mol%), respectively. The value of (G+C)/(A+T) was calculated as 0.78 for thermally denatured DNA sample, which coincided to the standard value of 0.77 [23].

4. Conclusions

In this work, a novel electrochemical sensor was fabricated based on AgNPs–Pdop@Gr modified GCE for the sensitive determination of guanine and adenine. AgNPs–Pdop@Gr nanocomposite was prepared with a simple and facile method by oxidation of dopamine at room temperature at Gr and subsequent electroless Ag deposition by mildly stirring. AgNPs–Pdop@Gr nanocomposite can greatly improve electron transfer between the analytes and underlying electrode. The developed biosensor based on AgNPs–Pdop@Gr nanocomposite exhibited wide linear detection range, acceptable reproducibility, good stability, and low detection limit. This novel as-prepared nanocomposite could provide a promising platform for the development of biosensor and electrochemical sensor.

Acknowledgments

This work was supported by the National Natural Science Foundation of China (21075106), Program for Science & Technology Innovation Talents in Universities of Henan Province (2010HASTIT025), and Excellent Youth Foundation of He'nan Scientific Committee (104100510020).

Appendix A. Supporting information

Supplementary data associated with this article can be found in the online version at http://dx.doi.org/10.1016/j.talanta.2013.04.017.

References

[1] F.Q. Yang, J. Guan, S.P. Li, Talanta 73 (2007) 269–273.
[2] Y. Fan, K.J. Huang, D.J. Niu, C.P. Yang, Q.S. Jing, Electrochim. Acta 56 (2011) 4685–4690.
[3] M.H. Yang, H. Li, A. Javadi, S.Q Gong, Biomaterials 31 (2010) 3281–3286.
[4] L. Zhou, L.J. Ou, X. Chu, G.L. Shen, R.Q. Yu, Anal. Chem. 79 (2007) 7492–7500.
[5] K.J. Huang, D.J. Niu, J.Y. Sun, C.H. Han, Z.W. Wu, Y.L. Li, X.Q. Xiong, Colloids Surf. B 82 (2011) 543–549.
[6] Z.H. Zhu, L.N. Qu, Q.J. Niu, Y. Zeng, W. Sun, X.T. Huang, Biosens. Bioelectron. 26 (2011) 2119–2124.
[7] H.B. Wang, T.T. Chen, S. Wu, X. Chu, R.Q. Yu, Biosens. Bioelectron. 34 (2012) 88–93.
[8] M. Zhou, Y. Zhai, S. Dong, Anal. Chem. 81 (2009) 5603–5613.
[9] C.L. Yang, Y.Q. Chai, R. Yuan, W.J. Xu, T. Zhang, F. Jia, Talanta 97 (2012) 406–413.
[10] H.F. Chen, D.P. Tang, B. Zhang, B.Q. Liu, Y.L. Cui, G.N. Chen, Talanta 91 (2012) 95–102.
[11] Q.X. Zhang, Q.Q. Ren, Y.Q. Miao, J.H. Yuan, K.K. Wang, F.H. Li, D.X. Han, L. Niu, Talanta 89 (2012) 391–395.
[12] H. Lee, S.M. Dellatore, W.M. Miller, P.B. Messersmith, Science 318 (2007) 426–430.
[13] F. Bernsmann, L. Richert, B. Senger, P. Lavalle, J.C. Voegel, P. Schaaf, V. Ball, Soft Matter. 4 (2008) 1621–1624.
[14] W. Hummers, R. Offeman, J. Am. Chem. Soc. 80 (1958) 1339–1340.
[15] J. Marmur, R. Rownd, C.L. Schildkraut, Progress in Nucleic Acid Research, Academic Press, New York 232.
[16] A.H. Kamel, F.T.C. Moreira, C. Delerue-Matos, M.G.F. Sales, Biosens. Bioelectron. 24 (2008) 591–599.
[17] J.C. Genereux, J.K. Barton, Chem. Rev. 110 (2010) 1642–1662.
[18] W. Sun, Y. Li, Y Duan, K. Jiao, Biosens. Bioelectron. 24 (2008) 988–993.
[19] F.W. Campbell, R.G. Compton, Anal. Bioanal. Chem. 396 (2010) 241–259.
[20] A. Abbaspour, A. Ghaffarinejad, Electrochim. Acta 55 (2010) 1090–1096.
[21] X. Tu, X. Luo, S. Luo, L. Yan, F. Zhang, Q. Xie, Microchim. Acta 169 (2010) 33–40.
[22] S. Shahrokhian, S. Rastgar, M.K. Amini, M. Adeli, Bioelectrochem 86 (2012) 78–86.
[23] T. Liu, X.B. Zhu, L. Cui, P. Ju, X.J. Qu, S.Y. Ai, J. Electroanal. Chem. 651 (2011) 216–221.